Int. J. Heat Mass Transfer. Vol. 1, pp. 280–293. Pergamon Press 1961. Printed in Great Britain.

MIXING AND CHEMICAL REACTION IN AN INITIALLY NON-UNIFORM TEMPERATURE FIELD*

S. I. CHENG and H. H. CHIU
Department of Aeronautical Engineering, Princeton University

(*Received* 10 *November* 1959; *revised* 8 *April* 1960)

Abstract—The development of the velocity, temperature and the concentration profiles in the vicinity of the trailing edge is investigated under the boundary layer approximation for an arbitrary initial temperature profile and an arbitrary value of the parameter B for the chemical kinetics.

A series solution is constructed in terms of a system of "universal functions", from which the initial development of an arbitrary initial temperature profile can be calculated with or without chemical reaction. The first three terms in the series for the temperature have been tabulated previously and are presented here in a diagram.

In the case of no chemical reaction, the analytical results for a given initial temperature distribution predict that the temperature gradient normal to the dividing stream line tends to increase for a limited distance in the downstream direction. This may not be anticipated from the consideration of thermal diffusion alone. Experimental results confirm this qualitative trend. With the three terms in the series solution for the temperature, the agreement between the analytical and the experimental results appears also quite satisfactory.

The analytical results will enable us to calculate the development of the temperature field with chemical reaction. There are as yet no experimental data for comparison.

Résumé—Le développement des profils de concentration, de température et de vitesse, au voisinage du bord de fuite, est étudié à partir d'une approximation de la couche limite pour un profil de température initial arbitraire et une valeur arbitraire du paramètre B de cinétique chimique.

Une solution en forme de série est donnée en fonction d'un système de "fonctions universelles" à partir de laquelle on peut calculer le développement d'un profil de température initial, avec ou sans réaction chimique. Pour la température, les trois premiers termes de la série ont été tabulés précédemment et sont présentés ici sous forme de diagramme.

Dans le cas où il n'y a pas de réaction chimique, les résultats analytiques, trouvés pour une distribution de température initiale, font prévoir un accroissement du gradient de température normal à la ligne de courant, à partir d'une certaine distance dans la direction aval. Ceci ne peut pas s'expliquer uniquement par la diffusion thermique. Les résultats expérimentaux confirment cette tendance qualitative. Avec trois termes de la série solution pour la température, l'accord entre résultats analytiques et expérimentaux semble tout à fait satisfaisant.

Les résultats analytiques nous permettent de calculer le développement du champ de température en présence de réaction chimique. Il n'y a pas encore de données expérimentales pour les comparer.

Zusammenfassung—In dieser Arbeit wird die Entwicklung der Profile der Geschwindigkeit, der Temperatur und der Konzentration in der Nähe der Anströmkante untersucht, wobei die Näherungen der Grenzschichtlehre sowie beliebige anfängliche Temperaturprofile und Werte für die Konstante B der chemischen Kinetik angenommen werden.

Es wird eine Reihenlösung in Ausdrücken eines Systems "universeller Funktionen" aufgestellt, von der aus die anfängliche Entwicklung eines willkürlichen anfänglichen Temperaturprofiles mit oder ohne chemische Reaktion berechnet werden kann. Die ersten drei Ausdrücke in den Reihen für die Temperatur wurden schon früher tabellarisch angegeben und sind hier in einem Diagramm mitgeteilt.

Für den Fall ohne chemische Reaktion zeigt das analytische Ergebnis für eine gegebene anfängliche Temperaturverteilung, dass der Temperaturgradient normal zur trennenden Stromlinie ansteigt für eine begrenzte Entfernung in Strömungsrichtung, was allein aus Betrachtungen über die Wärme

* This research is carried out as part of the work sponsored by the Office of Ordnance Research, U.S. Army under Contract No. OOR DA-36 ORD 2183.

ausbreitung nicht vorauszusehen war. Experimentelle Ergebnisse bestätigen qualitativ diesen Verlauf. Auch die drei Ausdrücke in der Reihenlösung für die Temperatur stimmen befriedigend mit dem Versuch überein.

Die analytischen Ergebnisse ermöglichen es, die Entwicklung des Temperaturfeldes mit chemischer Reaktion zu berechnen. Experimentelle Daten zum Vergleich liegen noch nicht vor.

Аннотация—Исследуется развитие полей скорости, температуры и концентрации вблизи задней кромки сепаратора при условии аппроксимации начального распределения температуры в пограничном слое и произвольной величины параметра B, характеризующего химическую кинетику.

Решение получено в виде ряда, состоящего из членов системы «универсальных функций», с помощью которого можно вычислить развитие произвольного температурного распределения при наличии химической реакции или без неё. Первые три члена ряда в решении для температурного поля были табулированы ранее и представлены здесь на диаграмме.

При отсутствии химической реакции аналитические результаты для данного начального температурного распределения показывают, что температурный градиент, перпендикулярный к линии, разделяющей потоки, стремится увеличиться на ограниченном расстоянии по направлению потока. Этого нельзя было бы ожидать, исходя из рассмотрения только термодиффузии.

Экспериментальные данные подтверждают этот качественный вывод. Аналитические и экспериментальные результаты также вполне удовлетворительно согласуются для решения, ограниченного тремя членами.

Аналитические результаты позволят вычислить развитие температурного поля при наличии химической реакции. Пока ещё нет экспериментальных данных для сравнения.

I. INTRODUCTION

IGNITION and combustion in the laminar mixing zone between a hot stream consisting of combustion products and a cool, combustible stream was first treated by Marble and Adamson [1] and continued by Dooley [6]. They considered a non-viscous, perfectly insulating, semi-infinite partition separating a cool combustible mixture from its hot combustion products. The velocity, temperature and concentration of combustible are assumed uniform in each half plane at the trailing edge of the partition. Their analysis gives the distribution of the temperature, the concentration of the combustible and the gas velocity in the neighborhood of the trailing edge of the partition. Their results indicate that a local maximum in the temperature profile first occurs, due to heat release by the chemical reaction, in the hot burned gas below the dividing stream line. The problem was reconsidered by Cheng and Kovitz in 1957 [2] to take into account the finite length of the partition and the viscosity of the gas. The initial velocity distribution is taken to be the Blasius flow over a flat plate, but the temperature of each stream is still taken as uniform and discontinuous across the thin partition. The results indicate that the development of the temperature and the velocity field is shortened by an order of magnitude as compared with the results of Marble and Adamson.

The key interest of the problem is to obtain an estimate of the distance of the local temperature maximum downstream of the trailing edge. This distance serves to represent the major coupling between the chemical kinetic and the fluid mechanical aspects in the problem of flame stabilization on a solid body [3]. In any practical system, heat transfer across the partition will give rise to a continuous temperature profile at the trailing edge. The heat transfer, prior to mass and momentum mixing in the wake may adversely affect the rate of chemical reaction and the associated phenomena as is clear from the discussions in [3].

The effect of a nonuniform, continuous initial temperature profile on the development of the wake of a combustible mixture will be considered in the present investigation.

The results of the present analysis brings out an interesting aspect of the heat transfer in a viscous wake layer. This is produced by the convective motion, normal to the partition, of the gases with nonuniform initial temperature profiles. The temperature gradient, normal to the partition, appears to increase in the downstream direction from the trailing edge of the partition for some limited extent. This prediction

from the analysis compares favorably with experimental results.

II. FORMULATION OF THE PROBLEM

The governing equations are the conservation laws of mass, momentum, energy and the concentration of the combustible. Subject to the appropriate assumptions [2], the Howarth transformation is employed to uncouple the continuity and the momentum equations from the energy and the diffusion equations. The momentum equation is then reduced to the incompressible form. In terms of the transformed variables the governing equations can be written as

$$\left.\begin{aligned} u_x + v_y &= 0 \\ uu_x + vu_y &= u_{yy} \end{aligned}\right\} \quad (1)$$

$$\left.\begin{aligned} u\theta_x + v\theta_y &= \frac{1}{Pr}\theta_{yy} + BK\exp\left(-\frac{\theta_a}{\theta}\right) \\ uK_x + vK_y &= \frac{1}{Sc}K_{yy} - CK\exp\left(-\frac{\theta_a}{\theta}\right) \end{aligned}\right\} \quad (2)$$

where Prandtl number $Pr = C_p\lambda/k$ and Schmidt number $Sc = \mu/\rho D$ are assumed to be constant throughout the field. The following notations are adopted from [2].

$B = 4l\Delta H/u_{I\gamma}\, C_pT_{II}$
$C = 4l/u_{I\tau}$
H = heat released per unit mass of combustible
τ = characteristic chemical time constant
R = universal gas constant
A = activation energy
K = relative mass concentration of combustible
T_{II} = heat stream temperature
$\theta = T/T_{II}$
$\theta_a = A/RT_{II}$

u and v are non-dimensional axial and transverse velocity components in the incompressible plane, while χ, y, are the corresponding non-dimensional co-ordinates with the origin at the trailing edge of the flat plate.

The solution for u and v from equations (1) was given by Goldstein [4] for the case of flow near the trailing edge of a flat plate with symmetric Blasius profile at the beginning of mixing.

With $\xi = \chi^{1/3} \quad \eta = y/3\xi$

The solution consists of two forms—one valid for y small and one for y large. For small y:

$$\left.\begin{aligned} u &= \tfrac{1}{3}\sum_{l=0}^{\infty} b_{3l+1}\,\xi^{3l+1} \\ v &= \tfrac{1}{3}\sum_{k=0}^{\infty} C_{3k-1}\,\xi^{3k-1} \end{aligned}\right\} \quad (3)$$

$$b_{3l+1} = f'_{3l}(\eta); \quad C_{3k-1} = \eta f'_{3k}(\eta) - (3k+2)f_{3k}(\eta)$$

The functions f_0, f_3, f_6, and their derivatives have been recalculated for smaller mesh size in [5] and are used in the present calculation.

Let the initial temperature profile be expressed in the power series form, for small y and $\bar{y}$ in the lower and the upper half plane respectively.

$$F(y) = \sum_{r=0}^{\infty}\beta_r\left(\frac{y}{3}\right)^r, \quad \bar{F}(\bar{y}) = \sum_{r=0}^{\infty}\bar{\beta}_r\left(\frac{\bar{y}}{3}\right)^r \quad (4)$$

The solution for $\theta(\xi_1\eta)$ will be constructed separately in the upper and lower half-planes. For small y, solutions of the forms

$$\theta(\xi\,.\,\eta) = \sum_{r=0}^{\infty}\theta_r(\eta)\xi^r, \quad K(\xi\,.\,\eta) = \sum_{r=0}^{\infty}K_r(\eta)\xi^r \quad (5)$$

are assumed in each plane. Terms of the type $\xi^r \ln \xi$ will be introduced before the ξ term whenever necessary.

The following limiting process is valid

$$\lim \sum_{r=0}^{\infty}\theta_r(\eta)\xi \to \sum_{r=0}^{\infty}\beta_r\left(\frac{y}{3}\right)^r$$

provided the limiting values

$$\lim_1 \frac{\theta_r(\eta)}{\eta^r} \to \beta_r, \quad \lim_2 \frac{\bar{\theta}_r(\bar{\eta})}{\bar{\eta}^r} = \bar{\beta}_r \quad (6)$$

exist for each θ_r and $\bar{\theta}_r$;

where

$$\lim_1 = \xi \to 0 \quad \eta \to \infty \quad y = \text{const.}$$

$$\lim_2 = \xi \to 0 \quad \bar{\eta} \to \infty \quad \bar{y} = \text{const.}$$

The constant β_r, $\bar{\beta}_r$ will be considered as given but will not be specified for the present analysis.

They will be determined from an experimentally measured initial profile.

The initial conditions for the concentration are

$$\lim_1 K(\xi \,.\, \eta) \to 0, \quad \lim_2 \bar{K}(\xi \,.\, \bar{\eta}) \to 1 \tag{7}$$

therefore

$$\left.\begin{aligned} &\lim_1 K_0(\xi \,.\, \eta) \to 0, \quad \lim \bar{K}_0(\xi \,.\, \bar{\eta}) \to 1 \\ &\lim_1 K_r(\xi \,.\, \eta)/\eta_r = \lim_2 \bar{K}_r(\xi \,.\, \bar{\eta})/\bar{\eta}_r \to 0 \end{aligned}\right\} \tag{8}$$

when β_0 is rather close to unity, the equation (4) for the initial temperature profile may be suitable for the expansion of the exponential terms in equation (2). (See Appendix A.) The results are summarized as follows

$$\exp\left(-\frac{\theta_a}{\theta}\right) = \sum_{j=0}^{\infty} D_j(\eta)\xi^j \tag{9}$$

where

$$\left.\begin{aligned} D_0 &= \exp\left(-\frac{\theta_a}{\beta_0}\right) \\ D_1 &= \left(\frac{\theta_a\theta_1}{\beta_0^2} + \frac{\beta_1\theta_a}{\beta_0^2}\,\eta\right)\exp\left(-\frac{\theta_a}{\beta_0}\right) \\ D_2 &= \left\{\left(\frac{\theta_a\theta_2}{\beta_0^2} + \frac{\beta_2\theta_a}{\beta_0^2} - \frac{\theta_a\theta_1^3}{\beta_0^3} + \frac{1}{2}\frac{\theta_a^2\theta_1^4}{\beta_0^4}\right) + \right. \\ &\quad + \left(\frac{\beta_1\theta_a}{\beta_0^4} - \frac{2\beta_1\theta_a}{\beta_0^3}\,\theta_2\right)\eta + \\ &\quad \left. + \left(\frac{1}{2}\frac{\theta_a}{\beta_0} - 1\right)\left(\frac{\theta_a}{\beta_0}\right)\left(\frac{\beta_1^2}{\beta_0}\right)\eta^2\right\}\exp\left(-\frac{\theta_a}{\beta_0}\right) \end{aligned}\right\} \tag{9a}$$

when β_0 is not close to unity, the series (9a) fails to be adequate since only three terms have been carried out for the solution of θ. An alternate expansion of the exponential term should be used. The series has the same form as equation (9) except that D_0, D_1, D_2, are now different from those in (9a). The new coefficients are

$$\left.\begin{aligned} D_0 &= \exp\left(-\frac{\theta_a}{Fm}\right) \\ D_1 &= \left(\frac{\theta_a\theta_1}{Fm^2}\,\alpha_0 + 3\alpha_1\eta\right)\exp\left(-\frac{\theta_a}{Fm}\right) \\ D_2 &= \left\{\alpha_0\theta_a\left[\left(\frac{\theta_a}{Fm^2} - \frac{\theta_1^3}{Fm^3}\right) + \frac{1}{2}\frac{\theta_1}{Fm^2}\right] + \right. \\ &\quad \left. + 3\alpha_1\theta_a\frac{\theta_1}{Fm^2}\,\eta + 3\alpha_2^2\eta^2\right\}\exp\left(-\frac{\theta_a}{Fm}\right) \end{aligned}\right\} \tag{9b}$$

where

$$\left.\begin{aligned} \alpha_0 &= 1 - \frac{\theta_a}{Fm^2}\,Fm'\,\delta m + \\ &\quad \frac{1}{2}\frac{\theta_a}{Fm^2}\left(Fm'' - \frac{2Fm'^2}{Fm} + \frac{\theta_a Fm'}{Fm^2}\right)\delta m^2 \\ \alpha_1 &= \frac{\theta_a}{Fm^2}\,Fm' - \frac{\theta_a}{Fm^2}\left(Fm'' - \right. \\ &\quad \left. - \frac{2Fm'^2}{Fm} + \frac{\theta_a Fm'^2}{Fm^2}\right)\delta m \\ \alpha_2 &= \frac{1}{2}\frac{\theta_a}{Fm^2}\left(Fm'' - \frac{2Fm'^2}{Fm} + \frac{\theta_a Fm'^2}{Fm^2}\right) \end{aligned}\right\} \tag{9c}$$

Substituting (3), (4) and (9) into (2), and equating the coefficients of like powers of ξ, we obtain a series of ordinary differential equations for $\theta_r(\eta)$ and $K_r(\eta)$ as were in [2].

The equations $\theta_r(r = 0, 1, 2, 3, 4)$, and $K_r(r = 0, 1, 2)$ are given as follows

$$\left.\begin{aligned} &\frac{1}{Pr}\,\theta_0'' + 2f_0\,\theta_0' = 0 \\ &\frac{1}{Pr}\,\theta_1'' + 2f_0\,\theta_1' - f_0'\,\theta_0' = 0 \\ &\frac{1}{Pr}\,\theta_2'' + 2f_0\,\theta_2' - 2f_0'\,\theta_2 = -9BD_0K_0 \\ &\frac{1}{Pr}\,\theta_3'' + 2f_0\,\theta_3' - 3f_0'\,\theta_3 = \\ &\quad - 9B(D_0K_1 + D_1K_0) - 5f_3\,\theta_0' \\ &\frac{1}{Pr}\,\theta_4'' + 2f_0\,\theta_4' - 4f_0'\,\theta_4 = -9B(D_0K_2 + \\ &\quad + D_2K_0) - 5f_3\,\theta_1' + f_3'\,\theta_1 + f_0'\,\theta_4 \\ &\frac{1}{Pr}\,\tilde{\theta}_4'' + 2f_0\,\tilde{\theta}_4 - 4f_0'\,\tilde{\theta}_4 = 0 \end{aligned}\right\} \tag{10}$$

$$\left.\begin{aligned} &\frac{1}{Sc}\,K_0'' + 2f_0K_0' = 0 \\ &\frac{1}{Sc}\,K_1'' + 2f_0K_1' - f_0'K_1 = 0 \\ &\frac{1}{Sc}\,K_2'' + 2f_0K_2' - 2f_0'K_2 = 9CD_0K_0 \end{aligned}\right\} \tag{11}$$

III. INTEGRATION OF θ AND K FOR SMALL y

The solution of the differential equations will, in general, depend on the imposed boundary conditions and the governing equation itself. For purposes of practical application of the solution to this problem for a given set of physical quantities and initial conditions, it is desirable to split the equation in several parts so that the individual equation can be freed from any arbitrary constants by suitable scale transformations. Such a splitting is permissible, since the equations for θ_r and K_r are linear. A complete solution can then be obtained by summing up the split equations.

(1) *The splitting of the solution*

There are no physical constants appearing in the homogeneous part of the differential equation except the Prandtl number and the Schmidt number which were assumed to be 0·75 and 1·00 respectively. The value of 0·75 assumed for the Prandtl number is based on the properties of CO_2 at high temperature. The Schmidt number is chosen according to the data of ethylene oxide and CO_2, the two components that will be used in the experiment. The homogeneous solution is split into two linearly independent solutions. Each solution is associated with an undetermined constant. The canonical boundary condition is assigned at $\eta = 0$, for each homogeneous solution. When the equation is non-homogeneous, the forcing function is split into several parts, in such a way that any physical constant, which appears in either part may be adsorbed in the appropriate scale transformations. Proper boundary values are assigned at $\eta = 0$, so that the numerical calculation will not lead to trivial solution.

Each split equation is then integrated separately with the given boundary value at $\eta = 0$, the integration process stops whenever each split equation reaches a substantially stable asymptotic region. The numerical values are tabulated in [7] and given graphically as Fig. 1. The process of splitting requires that an inordinately large number of independent solutions be integrated. For example, θ_3, $\bar{\theta}_3$, requires 6 integrations and θ_4, $\bar{\theta}_4$, requires 24 independent integrations. Only the integrations of θ_1, θ_2 and θ_3 have been carried out. Therefore, the present

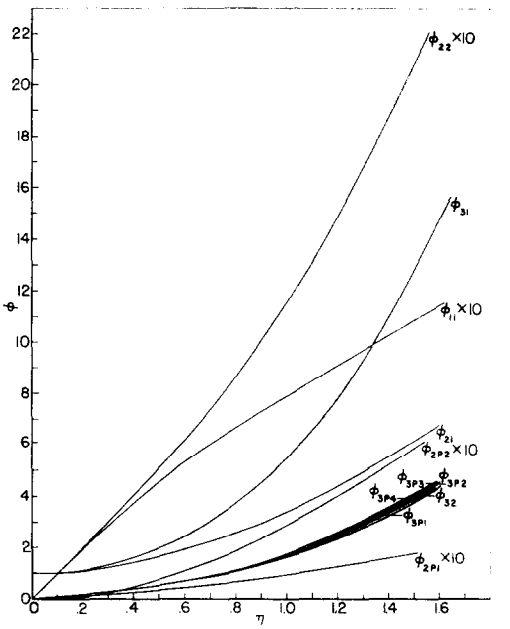

FIG. 1a. Curves of universal temperature function.

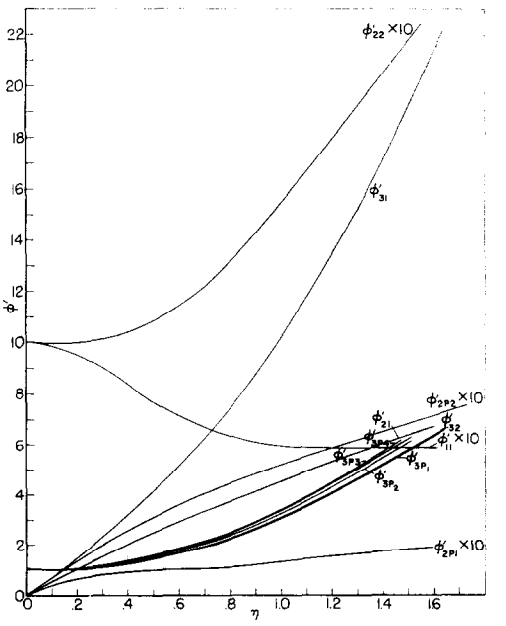

FIG. 1b. Derivative curve of universal temperature function.

solution cannot be extended to large values of χ and y.

(2) *Determination of the constants*

After each split solution is integrated, all the solutions are summed to construct a complete solution to a given physical problem.

There are four constants to be determined for each pair of θ_r, $\bar{\theta}_r$. Thus four boundary conditions are required, i.e., those at $\eta = \bar{\eta} = 0$ and $\eta = \bar{\eta} = \infty$. The condition that the temperature profile be smooth at any value of ξ requires that both the function and its first derivative be continuous at $\eta = 0$. At $\eta = \infty$, the temperature profile must approach the initial profile as a limit. This requires that equations (6) must be satisfied for all θ_r's. The asymptotic behaviors of θ_r and K_r, as specified by the differential equations are compatible with those specified in equations (6). The asymptotic behavior of the solution also serves to indicate the cut off point of the numerical integration. The investigation of the asymptotic behavior of θ_r, $(r = 0, 1, 2, 3, 4)$ is presented in Appendix B, and the results are tabulated in Table 1.

Table 1. *Asymptotic behaviour of* θ_r

r	I	$\theta^{(0)}_{\text{asy.}}$	$\theta^{(P)}_{\text{asy.}}$
0	0	η_1^0	
1	0	η_1^1	
2	$\eta_1^{-2} \exp\left(-\frac{P}{3}\eta_1^3\right)$	η_1^2	η_1^2
3	$\eta_1^{-2} \exp\left(-\frac{P}{3}\eta_1^3\right)$	η_1^3	η_1^3
4	η_1^5	η_1^4	$\eta_1 \ln \eta_1$
4	0	η^4	

Where I is the forcing functions appeared in equation (10). $\theta^{(0)}_{\text{asy.}}$ is the asymptotic behavior of homogeneous solution while $\theta^{(P)}_{\text{asy.}}$ is that of inhomogeneous solution with $\eta_1 = \eta + 0{\cdot}3408$.

The asymptotic behavior of θ_4 is $\eta_1^4 \ln \eta_1$, therefore θ_4 must include a term like $\xi^4 \ln \xi$.

Since the integrations have been carried out only to $r = 3$, the logarithmic term does not appear in the present expansion.

Numerical results for θ_0, θ_1, θ_2 and θ_3 are tabulated in [7] for $Pr = 0{\cdot}75$ and $Sc = 1{\cdot}0$.

The governing equations of K_0 and K_1 as well as their boundary conditions are identical to those in [2] and the solutions are applicable to the present analysis. Since K_2 does not appear in the governing equations for θ_0, θ_1, θ_2, θ_3, it has not been integrated.

(3) *The splitting of* θ_1

For illustrative purposes, the method of splitting and the determination of the constants will be given for the case of θ_1. The equation for θ_1, as given in equation (10) is invariant under the scale transformation,

$$\theta_1 = \beta_1 \Theta_1 \text{ and } \bar{\theta}_1 = \bar{\beta}_1 \bar{\Theta}_1$$

where $\beta_1 = -\bar{\beta}_1$ for the upper and the lower half plane respectively.

We split each of Θ_1 and $\bar{\Theta}_1$ into two independent solutions φ_{11}, and φ_{12} respectively

$$\left.\begin{aligned} \Theta_1 &= A_{11}\varphi_{11} + A_{12}\varphi_{12} \\ \bar{\Theta}_1 &= \bar{A}_{11}\varphi_{11} + \bar{A}_{12}\varphi_{12} \end{aligned}\right\} \tag{12}$$

so that

$$L_1 \varphi_{11} = 0, \quad L_1 \varphi_{12} = 0 \tag{13}$$

where

$$L_1 = \frac{\mathrm{d}}{\mathrm{d}\eta^2} + 2Pr f_0 \frac{\mathrm{d}}{\mathrm{d}\eta} - Pr f_0' \tag{14}$$

Subject to the canonical initial conditions

$$\left.\begin{aligned} \varphi_{11}(0) &= 0 \\ \varphi_{11}'(0) &= 1 \end{aligned}\right\}, \quad \left.\begin{aligned} \varphi_{12}(0) &= 1 \\ \varphi_{12}'(0) &= 0 \end{aligned}\right\} \tag{15}$$

The four unknown constants, A_{11}, A_{12}, $\bar{A}_{11}$ and $\bar{A}_{12}$ are to be determined by

(1) the initial conditions as given in equations (6) and

(2) the smooth matching of the function, and the first derivatives at $\eta = \bar{\eta} = 0$, i.e.

$$\beta_1 \Theta_1(0) = \bar{\beta}_1 \bar{\Theta}_1(0) \tag{16}$$

$$\beta_1 \Theta_1'(0) = -\bar{\beta}_1 \bar{\Theta}_1'(0) \tag{17}$$

These conditions of continuity require $A_{11} = \bar{A}_{11}$ and $A_{12} = -\bar{A}_{12}$. The case of

Table 2(a). *The split solution (when β_0 is close to unity)*
$\theta_r = Nr\ Ari\ \varphi ri + Nrp\ Arpi\ \varphi rp_i$

r		i	N	A	$\varphi(0)$	$\varphi'(0)$
1			β_1	C_{11}	0	1
1		2	β_1	0	0	0
2		1	1	$\{(\beta_2 + \bar{\beta}_2) - N_{2p}(C_{2p1} + C_{2p2})\}/2C_{21}$	1	0
2		2	1	$\{(\beta_2 - \bar{\beta}_2) - N_{2p}(C_{2p1} - C_{2p2})\}/2C_{22}$	0	1
2	p	1	$-9BPr \exp\left(-\frac{\theta_a}{\beta_0}\right)$	1	0	0
2	p	2	$-9BPr \exp\left(-\frac{\theta_a}{\beta_0}\right)$	1	0	0
3		1	1	$\{(\beta_3 + \bar{\beta}_3) - N_{3p}[C_{11}(C_{3p1} - C_{3p3}) - (C_{3p2} - C_{3p4})]\}/2C_{31}$	1	0
3		2	1	$\{(\beta_3 - \bar{\beta}_3) - N_{3p}[C_{11}(C_{3p1} + C_{3p3}) - (C_{3p2} + C_{3p4})]\}/2C_{32}$	0	1
3	p	1	$-9BPr \exp\left(-\frac{\theta_a}{\beta_0}\right)\frac{\theta_a\beta_1}{\beta_0^2}$	C_{11}	0	1
3	p	2	$-9BPr \exp\left(-\frac{\theta_a}{\beta_0}\right)\frac{\theta_a\beta_1}{\beta_0^2}$	1	0	1
3	p	3	$-9BPr \exp\left(-\frac{\theta_a}{\beta_0}\right)\frac{\theta_a\beta_1}{\beta_0^2}$	C_{11}	0	1
3	p	4	$-9BPr \exp\left(-\frac{\theta_a}{\beta_0}\right)\frac{\theta_a\beta_1}{\beta_0^2}$	1	0	1

In which $C_{ri} = \lim_{\eta \to \infty} \varphi_{ri}/\eta_r$
Subscript p indicates particular integral

Nr indicates the scale multiplier for θ_r
β_r the coefficient for the initial temperature profile.

Table 2(b). *The split solution (when β_0 is not close to unity)*

r		i	N	A	$\varphi(0)$	$\varphi'(0)$
1			β_1	C_{11}	0	1
1		2	β_1	0	0	0
2		1	1	$(\beta_2 + \bar{\beta}_2 - N_{2p}C_{2p1})/2C_{21}$	1	0
2		2	1	$(\beta_2 - \bar{\beta}_2 - N_{2p}C_{2p1})/2C_{22}$	0	1
2	p	1	$-9BPr \exp\left(-\frac{\theta_a}{Fm}\right)a_0$		0	0
2		2	0		0	0
3		1	1	$(\beta_3 + \bar{\beta}_3 - N_{3p1}C_{3p1} - N_{3p2}C_{3p2})/2C_{31}$	1	0
3		2	1	$\beta_3 - \bar{\beta}_3 - N_{3p1}C_{3p1} - N_{3p2}C_{3p2})/2C_{32}$	0	1
3	p	1	$-9BPr \exp\left(-\frac{\theta_a}{Fm}\right)\frac{\theta_a A_{11}a_0\beta_1}{Fm^2}$	C_{11}	0	1
3	p	2	$-9BPr \exp\left(-\frac{\theta_a}{Fm}\right)3a_1$	1	0	1
3	p	3	0		0	1
3	p	4	0		0	1

$A_{12} = -\bar{A}_{12}$ is ruled out by the antisymmetricity of θ_1 and $\bar{\theta}_1$. The initial conditions

$$\lim_{\eta\to\infty} \theta_1/\eta \to \beta_1, \quad \lim_{\bar{\eta}\to\infty} \bar{\theta}_1/\bar{\eta} \to \bar{\beta}_1 = -\beta_1 \tag{18}$$

lead to the same result

$$\lim_{\eta\to\infty} A_{11}\varphi_{11}/\eta \to 1 \tag{19}$$

therefore

$$A_{11} = \bar{A}_{11} = 1/\lim_{\eta\to\infty}(\varphi_{11}/\eta) \tag{20}$$

The integration of φ_{11} was carried out up to the point where φ_{11}/η, or φ'_{11} remains essentially constant. The numerical value of A_{11} or $\bar{A}_{11}$ is obtained from (20). The splitting procedure for the independent integrations, and the constants for each split solution are tabulated in Tables 2 (a, b).

IV. RESULTS AND DISCUSSION

(1) *Construction of complete solution of θ for small y and $\bar{y}$*

The complete solution for θ can be written in the following way with all the numerical results inserted:

$$\begin{aligned}\theta = \beta_0 &+ 1{\cdot}70\,\beta_1\varphi_{11}\xi + \Big\{\Big[0{\cdot}280\,(\beta_2 + \\ &+ \bar{\beta}_2) + 0{\cdot}562\,BPr\exp\left(-\frac{\theta_a}{\beta_0}\right)\Big]\varphi_{21} + \\ &+ \Big[0{\cdot}820\,(\beta_2 - \bar{\beta}_2) - 0{\cdot}900\,BPr \\ &\exp\left(\frac{-\theta_a}{\beta_0}\right)\Big]\varphi_{22} - 9BPr\exp\left(-\frac{\theta_a}{\beta_0}\right) \\ &\varphi_{2p1}\Big\}\xi^2 + \Big\{\Big[0{\cdot}270\,(\beta_3 + \bar{\beta}_3) - 0{\cdot}0453\,BPr \\ &\exp\left(-\frac{\theta_a}{\beta_0}\right)\frac{\theta_a\beta_1}{\beta_0^2}\Big]\varphi_{31} + \Big[0{\cdot}904\,(\beta_3 - \\ &- \bar{\beta}_3) + 4{\cdot}41\,BPr\exp\left(-\frac{\theta_a}{\beta_0}\right)\frac{\theta_a\beta_1}{\beta_0^2}\Big]\varphi_{32} - \\ &- 9BPr\exp\left(-\frac{\theta_a}{\beta_0}\right)\frac{\theta_a\beta_1}{\beta_0^2}(1{\cdot}710\,\varphi_{3p1} + \\ &+ \varphi_{3p2})\Big\}\xi^3 + \cdots\end{aligned} \tag{21}$$

$\bar{\theta}$ can be written in the same manner except that all the constant β_r must be properly modified and φ_{2p1}, φ_{3p1}, φ_{3p2}, must be replaced by φ_{2p2} φ_{3p3}, and φ_{3p4}. Thus the solutions for θ and $\bar{\theta}$ can be easily calculated at any point ξ, η within the range of validity of the series. Furthermore, the location of the initial bulge can be calculated by substituting the asymptotic solutions of φ_{ij}'s.

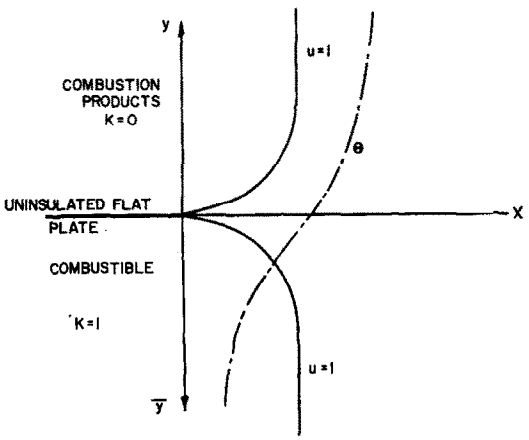

FIG. 2. Schematic of model with co-ordinate system.

(2) *Case of no chemical reaction*

The temperature distribution in the case of the mixing of a heated and a cold air stream, has been calculated for a particular initial temperature profile. The results are compared with the experiment as shown in Figs. 3 and 4.

Fig. 3 shows the initial velocity profile with the free stream velocity of approximately 15·2 ft/sec for both streams. (In Fig. 3 it is seen that the velocity profile is not symmetric with respect to the partition $y = 0$, as in the physical plane.

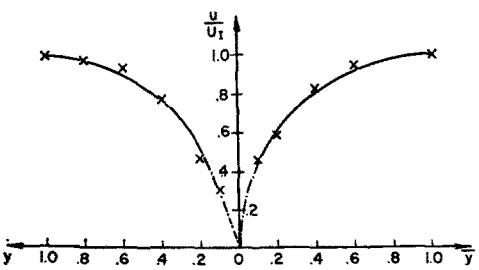

FIG. 3. Initial velocity profile in compressible plane.

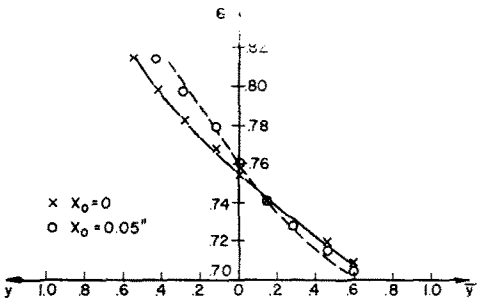

FIG. 4. Temperature profile incompressible plane.

When the y co-ordinates are contracted, according to the Howarth transformation, they will reduce to approximately symmetric Blasius profile as postulated in the analysis. The reduction of the experimental data will be given in Appendix C.) Fig. 4 shows the temperature distribution in the wake near the trailing edge. The free stream temperatures of the hot and the cold streams are 540° and 45°F respectively.

In Fig. 4 the cross represents the initial temperature as measured. The solid curve is the approximation for the initial temperature profile on which the calculation of the downstream flow field is based.

The circle represents the temperature measured at different transverse positions, 0·05 in. downstream of the trailing edge. The broken line is the corresponding temperature distribution as calculated based on equation (21).

It is interesting to note from both the measured and the calculated profile that the downstream temperature is higher than the upstream temperature in the hot stream side, and is lower in the cold stream side along constant y lines when $|y|$ is small. As a result, the temperature profile shows a steeper slope toward the downstream region along the dividing stream line.

This result might be disturbing if one should consider the change of temperature distribution as being carried out by the diffusive process alone as in the ideal case of mixing of two uniform streams.

However, inside the viscous mixing region of two uniform streams, the stream lines must converge toward the dividing stream line immediately downstream of the trailing edge of the partition. This is because the u-velocity component parallel to the dividing stream line, increases toward the downstream direction, i.e. $\partial u/\partial x > 0$. The equation of mass continuity then gives

$$\frac{\partial v}{\partial y} = -\frac{\partial u}{\partial x} + \frac{1}{\rho}\frac{\mathrm{D}\rho}{\mathrm{D}t}.$$

While $\partial u/\partial x$ becomes very large, $-(1/\rho)(\mathrm{D}\rho/\mathrm{D}t)$ is vanishingly small when the trailing edge is approached. Hence $\partial v/\partial y < 0$. With $v = 0$ at $y = 0$ the transverse velocity component v is always negative. The stream lines will therefore converge inside the viscous wake layer, at least immediately downstream of the trailing edge.

The convergence of the stream lines on both sides of the partition toward $y = 0$, upon entering into the wake, tends to increase the temperature gradient across the dividing stream line $y = 0$. This is opposite to the effect of heat diffusion. If the former effect predominates the temperature gradient across the stream line will actually increase toward the downstream region as was found from both the calculated and the measured results. The importance of the non-uniform initial temperature profiles in each stream in determining the temperature field in the wake, especially near the trailing edge of the partition, is then evident even in the absence of chemical reaction.

(3) *Case with chemical reaction*

The rate of chemical reaction in the wake region will be adversely affected because of the lowered effective temperature over the hot side of the wake. However, no definite conclusion could be made concerning the development of the maximum in the temperature profile. The effect of the lowered rate of chemical kinetics is counteracted by the lower rate of heat transfer from the hot stream to the cold stream. Moreover, the maximum temperature point developed deeper in the hot stream when compared with the case with step initial temperature profile. It is difficult to visualize qualitatively how the overall effect will be in the presence of these opposing influences. A detailed investigation will have to depend on the calculated results for specific instances based on equation (21a).

The criteria of the initial maximum in temperature profile is given as [2]:

$$\theta_\eta = \theta_{\eta\eta} = 0 \tag{22}$$

θ_η and $\theta_{\eta\eta}$ are calculated from the complete solution (21a) by substituting asymptotic approximation in φ_{ipj}. The asymptotic approximation of φ_{ipj} are given in Appendix D. The results are

$$\theta_\eta = (\beta_1 + \tfrac{2}{3}\beta_2 y + a_{22}\chi^{1/3} + \tfrac{1}{3}\beta_3 y^2 + \tfrac{1}{3}a_{32} y\chi^{1/3} + a_{33}\chi^{2/3})(\chi^{1/3}) \tag{23}$$

$$\theta_{\eta\eta} = (\tfrac{2}{3}\beta_2 + \tfrac{2}{3}\beta_3 y + \tfrac{1}{3}a_{32}\chi^{1/3})(3\chi^{2/3}) \tag{24}$$

where

$$\left.\begin{aligned} a_{22} &= 0{\cdot}559\,\beta_2 - 0{\cdot}003\,\beta_2 + \\ &\quad + 0{\cdot}009\,BPr\exp\left(-\frac{\theta_a}{Fm}\right)\alpha_0 \\ a_{32} &= 2{\cdot}321\,\beta_3 + 0{\cdot}023\,\beta_3 - \\ &\quad - 9BPr\exp\left(-\frac{\theta_a}{Fm}\right)\left(5{\cdot}150\,\frac{\theta_a A_{11}\beta_1}{Fm^2}\alpha_0 + \right. \\ &\quad \left. + (5{\cdot}468)3\alpha_1\right) \\ a_{33} &= 0{\cdot}076\,\beta_3 - 0{\cdot}068\,\beta_3 + \\ &\quad + 9BPr\exp\left(-\frac{\theta_a}{Fm}\right)\left(3{\cdot}043\,\frac{\theta_a A_{11}\beta_1}{Fm^2}\alpha_0 + \right. \\ &\quad \left. + (3{\cdot}436)3\alpha_1\right) \end{aligned}\right\} \tag{25}$$

The co-ordinates of the location with the initial maximum in the temperature profile are found from (22–24) as

$$\chi_i^{1/3} = \frac{\{-2(a_{32}\beta_2 - 3a_{22}\beta_3)\,[1 + \sqrt{1 - (\beta_2^2 - 3\beta_1\beta_3)(a_{32}^2 - 12\beta_3 a_{33})/(a_{32}\beta_2 - 3a_{22}\beta_3)^2}]\}}{(a_{32}^2 - 12\beta_3 a_{33})} \tag{26}$$

$$y_i = \frac{-(a_{32}\chi_i^{1/3} + 2\beta_2)}{2\beta_3} \tag{27}$$

After substituting expressions (25) in equation (26) one obtains a general formula for $\chi_i^{1/3}$, which will be extremely complicated. However, it can be expanded in power series of the small parameter $[9BPr\exp(-\theta_a/Fm)]$ provided the following assumptions are satisfied:

(i) $\left|3\frac{a_{22}}{a_{32}}\frac{\beta_3}{\beta_2}\right| < 1$

(ii) $\left|\frac{2[1 - (3\beta_1\beta_3/\beta_2^2)]\beta_2/\beta_1}{a_{32}}\left(a_{22} - 2\frac{a_{33}}{a_{32}}\right)\right| < 1$

These are satisfied under typical conditions. For example, for the case reported in [2] with

$B = 2{\cdot}58 \times 10^{13}$, $\theta_a = 23{\cdot}96$, $Fm = 0(1)$
$\delta m = 0(1)$

The first terms of the expansions are

$$\chi_i^{1/3} = \frac{\beta_2 + \sqrt{(3\beta_1\beta_3)}}{8{\cdot}20\,\alpha_1\,[1 + 0{\cdot}314\,(\theta_a\beta_1/Fm^2)\,(\alpha_0/\alpha_1)]} \times \left\{1 - \frac{0{\cdot}001}{16{\cdot}40\,\alpha_1\,[1 + 0{\cdot}314\,(\theta_a\beta_1/Fm^2)\,(\alpha_0/\alpha_1)]}\right\} \times \frac{1}{9BPr\exp(-\theta_a/Fm)} \tag{28}$$

$$y_i = \sqrt{\frac{3\beta_1}{\beta_3}} \times \left[1 - \frac{0{\cdot}003\,\alpha_0\theta_a}{16{\cdot}40\,\alpha_1}\,\frac{\beta_2 + \sqrt{(3\beta_1\beta_3)}}{1 + 0{\cdot}314\,(\theta_a\beta_1/Fm^2)\,(\alpha_0/\alpha_1)}\right] \tag{29}$$

when the second term in the brackets in equations (28) and (29) is small compared to unity. y_i is approximately equal to $\sqrt{(3\beta_1/\beta_3)}$. $\alpha_0\alpha_1$ etc. will then be evaluated at $\delta m = \sqrt{(3\beta_1/\beta_3)}$. By substituting these values into equations (28) and (29) one obtains a point of the initial maximum in temperature profile.

The increase in temperature at χ_i, y_i due to the chemical heat generation can be calculated from equation (21a) as follows

$$\Delta\theta = 0{\cdot}696\,[\beta_2 + \sqrt{(3\beta_1\beta_3)}]\left(\frac{3\beta_1}{\beta_3}\right)\left\{1 + 0{\cdot}455\,\frac{\theta_a\beta_1}{Fm^2}\frac{\alpha_0}{\alpha_1} + 0\left[\frac{\theta_a\beta_1}{Fm^2}\frac{\alpha_0}{\alpha_1}\right]^2 + \ldots\right\}$$

It is interesting to note that both $\chi_i^{1/3}$, and $\Delta\theta_i$ are proportional to $[\beta_2 + \sqrt{(3\beta_1\beta_3)}]$ which is the second derivative of the initial temperature profile evaluated at $y = \sqrt{(3\beta_1/\beta_3)}$.

This result indicates that for larger negative curvature at y_i the greater is the distance required to develop the temperature maximum in agreement with physical expectations.

Typical values of β's and α's have been estimated from reasonable initial temperature profiles. Both the co-ordinates (χ_i y_i) of the point where temperature maximum occurs are found to be

$$\chi_i^{1/3} = 0{\cdot}0077 \quad . \quad y_i = 0{\cdot}485$$

when the physical constants given in [2] were adopted. Comparison with the values of $\chi_i^{1/3}$ and y_i given in [2] for the step initial temperature profile shows that the temperature maximum develops considerably further away from the dividing stream line and into the hot gas stream when the experimental, smooth initial temperature profile is used. The temperature maximum develops further upstream for the present case.

In conclusion, the present work presents an analytical method for calculating the temperature field with or without chemical reactions in the wake of a flow with nonuniform initial temperature. The importance of the nonuniformity of the initial temperature is illustrated by calling to the attention that the qualitative behavior of the immediate development of the temperature field is opposite to what may be expected if the nonuniformity is ignored. This qualitative analytic prediction is confirmed by experimental data. In view of the importance of the temperature field on the rate of chemical reaction, it is pertinent to emphasize the importance of the temperature nonuniformity in many practical problems, involving chemical reaction. A typical example is presented.

REFERENCES

1. F. E. MARBLE and T. C. ADAMSON, *Jet Propulsion* **24**, 85 (1954).
2. S. I. CHENG and A. A. KOVITZ, *J. Fluid Mech.* **4**, Part 1, 64 (1958).
3. S. I. CHENG and A. A. KOVITZ, *7th Combustion Symposium*, p. 681 (1958).
4. S. GOLDSTEIN, *Proc. Camb. Phil. Soc.* **26**, 1 (1930).
5. A. A. KOVITZ, *Ignition in the Laminar Wake of a Flat Plate*. Ph.D. Thesis, Department of Aeronautical Engineering, Princeton University (1956).
6. D. A. DOOLEY, *Combustion in Laminar Mixing Regions and Boundary Layers*. Ph.D. Thesis, California Institute of Technology (1956).
7. S. I. CHENG and H. H. CHIU, *Aerodynamics of Flame Stabilization*. 14th Quarterly Progress Report, Aeronautical Engineering Report No. 335-n, Princeton University.

APPENDIX A

Expansion of $\exp(-\theta_a/\theta)$

Expansion of $\exp(-\theta_a/\theta)$ about $\xi = 0$, holding y constant, can be written as:

$$\exp\left(\frac{-\theta_a}{\theta}\right) = \exp\left(-\frac{\theta_a}{\theta}\right)\Big|_{\xi=0} + \frac{\partial}{\partial\xi}\exp\left(\frac{-\theta_a}{\theta}\right) + \frac{1}{2!}\frac{\partial^2}{\partial\xi^2}\exp\left(-\frac{\theta_a}{\theta}\right)\Big|_{\xi=0}\xi^2 \quad \text{(A1)}$$

where

$$\exp\left(-\frac{\theta_a}{\theta}\right)\Big|_{\xi=0} = \exp\left(-\frac{\theta_a}{F(\eta,\,\xi)}\right)$$

since

$$\theta = F \text{ at } \begin{cases} \xi = 0 \\ \eta \to \infty \\ y = \text{const.} \end{cases}$$

$$\frac{\partial}{\partial\xi}\exp\left(-\frac{\theta_a}{\theta}\right)\Big|_{\xi=0} = \frac{\theta_a}{\theta^2}\theta_\xi \exp\left(-\frac{\theta_a}{\theta}\right)\Big|_{\xi=0} = \frac{\theta_a\theta_1}{F^2}\exp\left(\frac{-\theta_a}{F}\right)$$

Hence equation (1) can be written as

$$\exp\left(-\frac{\theta_a}{\theta}\right) = \exp\left(-\frac{\theta_a}{F}\right)\left\{1 + \xi\frac{\theta_a\theta_1}{F^2} + \xi^2\left[\theta_a\left(\frac{\theta_2}{F^2} - \frac{\theta_1^2}{F^3}\right) + \frac{1}{2!}\left(\frac{\theta_a\theta_1}{F^2}\right)\right] + \ldots\right\} \quad \text{(A2)}$$

$$F = \beta_0 + \beta_1\left(\frac{y}{3}\right) + \beta_2\left(\frac{y}{3}\right)^2 + \beta^3\left(\frac{y}{3}\right)^3 + \ldots$$

when β_0 is close to unity, the expansion of $\exp(-\theta_a/F)$ can be carried out about $y = 0$, with $y = 3\xi\eta$.

$$\left.\begin{aligned} &\exp\left(-\frac{\theta_a}{F}\right) = \exp\left(-\frac{\theta_a}{\beta_0}\right) + \\ &+ \frac{\beta_1\theta_a}{\beta_0^2}\exp\left(-\frac{\theta_a}{\beta_0}\right)\eta\xi + \\ &+ \left\{\frac{\beta_2\theta_a}{\beta_0^2} + \left[\frac{1}{2}\left(\frac{\theta_a\beta_1}{\beta_0^2}\right)^2 - \frac{\theta_a}{\beta_0}\left(\frac{\beta_1}{\beta_0}\right)^2\right]\right\} \times \\ &\times \exp\left(-\frac{\theta_a}{\beta_0}\right)\eta^2\xi^2 + \ldots + \\ &+ \frac{\beta_4\theta_a}{\beta_0^2}\exp\left(-\frac{\theta_a}{\beta_0^2}\right)\eta^4\xi^4 \ln\xi + \ldots \end{aligned}\right\} \quad \text{(A3)}$$

Substitute (A3) into (A2) and rearrange the result in ascending powers of ξ. The following series is obtained:

$$\left.\begin{aligned}
&\exp\left(-\frac{\theta_a}{\theta}\right) = \exp\left(-\frac{\theta_a}{\beta_0}\right) + \left(\frac{\theta_a\beta_1}{\beta_0^2}\eta + \right.\\
&+ \frac{\theta_a\theta_1}{\beta_0^2}\exp\left(\frac{\theta_a}{\beta_0}\right)\xi + \left\{\left(\frac{\theta_a\theta_2}{\beta_0^2} - \frac{\theta_a\theta_1^3}{\beta_0^2} + \right.\right.\\
&+ \frac{1}{2}\frac{\theta_a^2\theta_1}{\beta_0^2} + \frac{\theta_a^1\beta_2}{\beta_0^2}\Big) + \left(\frac{\theta_a^2\beta_1}{\beta_0^4} - \frac{2\theta_a\beta_1}{\beta_0^3}\theta_2\right)\eta + \\
&+ \left(\frac{1}{2}\frac{\theta_a}{\beta_0} - 1\right)\left(\frac{\theta_a}{\beta_0}\right)\left(\frac{\beta_1^2}{\beta_0}\right)\eta^2\Big\}\\
&\exp\left(-\frac{\theta_a}{\beta_0}\right)\xi^2 + \\
&+ \frac{\theta_a + \beta_4}{\beta_0^2}\exp\left(-\frac{\theta_a}{\beta_0}\right)\eta^4\xi^4\ln\xi + \ldots
\end{aligned}\right\} \quad (A4)$$

When β_0 is substantially different from unity, say 1/2, the above expansion cannot be used. The expansion of exp $(-\theta_a/F)$ must be such as to represent with reasonable accuracy this function in the region of y which is important in the development of the temperature maximum. The method of solution of the different equation regimes, on the other hand, exp $(-\theta_a/F)$ must be expressed in the form of power series of y. Hence assume the following expansion

$$\exp\left(-\frac{\theta_a}{F}\right) = \exp\left(-\frac{\theta_a}{Fm}\right)(\alpha_0 + \alpha_1 y + \\ + \alpha_2 y^2 + \ldots) \quad (A5)$$

α_0, α_1, and α_2, are so determined that the truncated polynomial will give the same zeroth. First and second derivatives of exp $(-\theta_a/F)$ at some important point $y = \delta m$. Hence,

$$\alpha_0 + \alpha_1\delta m + \alpha_2\delta m^2 = 1 \quad (A6)$$

$$\alpha_1 + 2\alpha_2\delta m = \left(\frac{\theta_a}{Fm^2}\right)Fm' \quad (A7)$$

$$2\alpha_2 = \frac{\theta_a}{Fm^2}Fm'' - \frac{2\theta_a}{Fm^3}(Fm')^2 + \frac{\theta_a^2}{Fm^4}(Fm')^2 \quad (A8)$$

From (A6), (A7) and (A8), α_0, α_1, α_2, are calculated, finally (A2) may be written as

$$\exp\left(-\frac{\theta_a}{F}\right) = \exp\left(-\frac{\theta_a}{Fm}\right)_1\Big[\alpha_0 + \Big(\alpha_0\frac{\theta_a\theta_1}{Fm^2} + \\ + 3\alpha_1\eta\Big)\xi + \Big\{\alpha_0\Big[\theta_a\Big(\frac{\theta_2}{Fm^2} - \frac{\theta^3}{Fm^3}\Big) + \\ + \frac{1}{2}\frac{\theta_a\theta_1}{Fm^2}\Big] + 3\alpha_1\frac{\theta_a\theta_1}{Fm^2}\eta + 3^2\alpha_2\eta^2\Big\}\xi^2 + \ldots\Big]$$

where

$$\alpha_0 = 1 - \frac{\theta_a}{Fm^2}Fm'\delta m + \frac{1}{2}\frac{\theta_a}{Fm^2}\Big(Fm'' - \\ - \frac{2Fm'^2}{Fm} + \frac{\theta_aFm'^2}{Fm^2}\Big)\delta m^2$$

$$\alpha_1 = \frac{\theta_a}{Fm^2}Fm' - \frac{\theta_a}{Fm^2}\Big(Fm'' - \\ - \frac{2Fm'^2}{Fm} + \frac{\theta_aFm'^2}{Fm^2}\Big)\delta m$$

$$\alpha_2 = \frac{1}{2}\frac{\theta_a}{Fm^2}\Big(Fm'' - \frac{2Fm'^2}{Fm} + \frac{\theta_aFm'^2}{Fm^2}\Big)$$

APPENDIX B

Asymptotic solution of $\theta_r^{(0)}$

The general equation for $\theta_r(\eta)$ can be written in the more convenient form

$$\theta_r'' + \lambda_2 f_0\theta_r' - \lambda_r f_0'\theta_r = Pr\, I_r$$

where

$$\lambda_r = rPr$$

$$I_0 = I_1 = \tilde{I}_4 = 0$$

$$I_2 = -9BD_0K_0$$

$$I_3 = -9B(D_0K_1 + D_1K_0)$$

$$I_4 = -9B(D_0K_2 + D_2K_0) - 5f_3\theta_1' + f_3'\theta_1 + f_0'\tilde{\theta}_4$$

The formal solution for θ_r can be written as

$$\theta_r(\eta) = a_rf_1^{(r)}(\eta) + b_rf_2^{(r)}(\eta) - \\ - Pr\int^\eta I_r\exp\left[-\lambda_2\int^\delta f_0(z)dz\right]\{f_2^{(r)}(\eta)f_1^{(r)}(\delta) - \\ - f_1^{(r)}(\eta)f_2^{(r)}(\delta)\}\,d\delta$$

where a_r, b_r are the arbitrary constants and $f_1^{(r)}$, $f_2^{(r)}$, are linearly independent solutions to the homogeneous equation. For large η Goldstein shows that f_0 behaves as quadratic function of η

$$f_0(\eta) \sim \tfrac{1}{2}\,\alpha_1\,(\eta + \delta_0)^2 + O[(\eta + \delta)^{-4} \exp\{-\alpha_1/3\,(\eta + \delta_0)^3\}]$$

$$f_0'(\eta) \sim \alpha_1\,(\eta + \delta_0)$$

Using these forms for f_0, f_0', the homogeneous equation becomes

$$\theta^{(0)} + \lambda_2\,\tfrac{1}{2}\,\alpha_1\,(\eta + \delta_0)^2\,\theta_r^{(0)} - - \lambda_2\alpha_1(\eta + \delta_0)\,\theta_r^{(0)} = 0$$

The solutions are

$$\theta_r^{(0)} \sim Ar\,\eta_1^{-r-2} \exp\left(-\frac{a}{3}\eta_1^3\right)$$

$$\left\{1 + \sum_{n=1}^{\infty}\left[\frac{1}{36} - \left(\frac{r+1}{3} + \frac{1}{2}\right)^2\right]\left[\frac{1}{36} - \left(\frac{r+1}{3} + \frac{3}{2}\right)^2\right], \left[\frac{1}{36} - \left(\frac{r+1}{3} + n - \frac{1}{2}\right)^2\right] \Big/ \left[n!\left(\frac{a}{3}\eta_1^3\right)^n\right]\right\}$$

$$+ B_r\eta_1^r\left\{1 + \sum_{n=1}^{\infty}\left[\frac{1}{36} - \left(-\frac{r+1}{3} + \frac{1}{2}\right)^2\right]\left[\frac{1}{36} - \left(-\frac{r+1}{3} + \frac{3}{2}\right)^2\right] \cdots \left[\frac{1}{36} - \left(\frac{r+1}{3} - - n + \frac{1}{2}\right)^2\right] \Big/ \left[(n!)\,(-1)^n\left(\frac{a}{3}\eta_1^3\right)^n\right]\right\}$$

where

$$\eta_1 = +\eta = \delta_0 + 0{\cdot}3408.$$

APPENDIX C

Reduction of experimental data

The velocity and temperature distribution, as shown in Figs. 3 and 4 are obtained at planes perpendicular to the free stream direction and located at $x = 0$ and $x = 0{\cdot}05$ in., respectively, as measured from the trailing edge of the plate. The hot air was heated by the electric heater to a temperature of 540°F while the cold air was observed to have a temperature of 45°F. Both free stream velocities were 15·2 ft/sec approximately.

The temperature distribution at $x = 0{\cdot}05$ in. was calculated analytically on the basis of equation (21) for a given set of values of β_r, and $\bar{\beta}_r$ which are determined by the initial temperature profile, in the following manner.

Firstly, the physical plane is transformed into the incompressible plane according to the Howarth transformation. For the constant pressure process, the density ratio ρ/ρ_I appearing in the transformation is replaced by the temperature ratio T_I/T. The compressible plane is thus transformed into the incompressible plane. To calculate the spatial variables $\chi = x_1/4l$, $y = \sqrt{(R)}y_1/4l$, as were defined by Goldstein, the effective flat plate length l must be estimated.

It may be obtained on the basis of either the formula of skin friction or of the expression of the change of the centerline velocity given by Goldstein [4]. The Blasius skin friction formula is

$$\left.\frac{\partial u}{\partial y_1}\right|_{y_1=0} = 0{\cdot}664\,\frac{Re^{1/2}}{4l}$$

where Re = Reynolds number $4lu_I/\nu$, l = effective length of the flat plate, u_I = free stream velocity in the direction parallel to the plate, y_1 = transverse distance co-ordinate in the incompressible plane. With $u_I = 15{\cdot}2$ ft/sec, $\nu = 1{\cdot}55 \times 10^{-4}$ ft²/sec., and with

$$\left.\frac{\partial u}{\partial y_1}\right|_{y_1=0} = 26{\cdot}3\ \text{in}^{-1}$$

as was obtained from the velocity profiles in the incompressible plane, l was found to be 1·30 in. Goldstein's formula for the centerline velocity is

$$u = \tfrac{1}{3}\sum_{r=0}^{\infty}\xi^{3r+1}f_{3r}'(0)$$

$f'(0) = 3{\cdot}67896$, $f_3'(0) = 3{\cdot}5415$, $f_6'(0) = 8{\cdot}1190$, with $u_I = 15{\cdot}2$ ft/sec, the centerline velocity distribution was found to fit well with that given with $l = 1{\cdot}25$ in. With $u_I = 15{\cdot}7$ ft/sec, l was found to be 0·8 in., these are shown in Fig. 5.

In the figure circles and crosses indicate the actual velocity distribution along the centerline with $u_I = 15{\cdot}2$ ft/sec and 15·7 ft/sec, respectively. The variation of the center velocity with $l = 1{\cdot}25$ in., 1·0 in., 0·8 in. are plotted. Weighing all the aspects involved, we decide to take $l = 1{\cdot}0$ in. in the calculation. The initial temperature profile in the x–y plane was approximated by

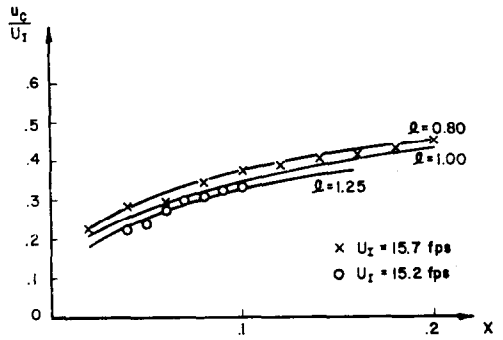

FIG. 5. Centerline velocity profile.

cubic equations for y and $\bar{y}$ smoothly joined at $y = \bar{y} = 0$. By taking 3 points in each y and $\bar{y}$ plane, the 6 unknown constants β_0, β_1, β_2, β_3, $\bar{\beta}_1$, $\bar{\beta}_2$, $\bar{\beta}_3$, are determined, where $\beta_1 = -\bar{\beta}_1$ is imposed as the necessary condition of smooth joining.

At $\chi_0 = 0{\cdot}05$ in., we have $\chi = 0{\cdot}0125$ and $\xi = 0{\cdot}232$. With the values $\beta_0 \ldots \bar{\beta}_3$ determined from the initial temperature profile, the corresponding temperature distribution at $\chi_0 = 0{\cdot}05$ in. is given by equation (21) as

$$\theta = 0{\cdot}7537 + 0{\cdot}0988\varphi_{11} + 0{\cdot}0119\varphi_{21} - \\ -0{\cdot}0301\varphi_{22} - 0{\cdot}004\varphi_{31} + 0{\cdot}0285\varphi_{32}$$

$$\bar{\theta} = 0{\cdot}7537 - 0{\cdot}0988\varphi_{11} + 0{\cdot}0119\varphi_{21} + \\ + 0{\cdot}0301\varphi_{22} - 0{\cdot}004\varphi_{31} - 0{\cdot}0285\varphi_{32}$$

Here φ's are functions of $\eta = y/3\epsilon$. For any given value of y, say $y = 0{\cdot}174$ $\eta = y/3\epsilon = 0{\cdot}25$ the following values are obtained from Table 2(b).

$$\varphi_{11} = 0{\cdot}2436, \quad \varphi_{21} = 1{\cdot}1598, \quad \varphi_{22} = 0{\cdot}2503, \\ \varphi_{31} = 1{\cdot}243, \quad \varphi_{32} = 0{\cdot}2570$$

Thus θ and $\bar{\theta}$ were calculated to be 0·7864, and 0·7387 respectively at the point $\eta = \bar{\eta} = 0{\cdot}25$.

The slope of the temperature profile along the stream line can be calculated easily by differentiating equation (21), with respect to y. With the present data the analytical result gave $\theta_y/\beta_1 = 1{\cdot}625$. While the experimental result is $1{\cdot}61\pm$ at $\xi = 0{\cdot}232$.

APPENDIX D

Asymptotic approximation of φ_{ipj}

The asymptotic expression of φ_{ipj} are approximated based on the computed values of the temperature function in [7] and are shown in the following:

$$\varphi_{11} = 0{\cdot}587\eta + 0{\cdot}200$$

$$\varphi_{21} = 1{\cdot}800\eta^2 + \eta + 0{\cdot}580$$

$$\varphi_{22} = 0{\cdot}610\eta^2 + 0{\cdot}343\eta + 0{\cdot}193$$

$$\varphi_{2p1} = 0{\cdot}052\eta^2 + 0{\cdot}028\eta + 0{\cdot}019$$

$$\varphi_{2p2} = 0{\cdot}173\eta^2 + 0{\cdot}167\eta - 0{\cdot}052$$

$$\varphi_{31} = 1{\cdot}850\eta^3 + 2{\cdot}170\eta^2 + 0{\cdot}015\eta + 1{\cdot}620$$

$$\varphi_{32} = 0{\cdot}553\eta^3 + 0{\cdot}635\eta^2 + 0{\cdot}080\eta + 0{\cdot}370$$

$$\varphi_{3p1} = 0{\cdot}095\eta^3 + 2{\cdot}680\eta^2 + 3{\cdot}010\eta + 1{\cdot}851$$

$$\varphi_{3p2} = 0{\cdot}100\eta^3 + 2{\cdot}850\eta^2 - 3{\cdot}300\eta + 2{\cdot}041$$

$$\varphi_{3p3} = 0{\cdot}103\eta^3 + 2{\cdot}930\eta^2 - 2{\cdot}847\eta + 1{\cdot}542$$

$$\varphi_{3p4} = 0{\cdot}105\eta^3 + 2{\cdot}979\eta^2 - 2{\cdot}911\eta + 0{\cdot}650$$

The above approximate expressions are justified from the point of view of the behavior of the asymptotic solution as is given in Appendix B.